Proposal For Beamtest of Hall D Forward Calorimeter Prototype Underneath Hall B Tagger

Kei Moriya*
Matthew Shepherd†
Indiana University Department of Physics

August 15, 2011

1 Introduction

The Forward Calorimeter (FCAL) of the GlueX detector will be an essential instrument in reconstructing many of the multi-particle final states that are expected to be produced in the GlueX Experiment. In this document we outline a proposal to test a prototype of the Forward Calorimeter underneath the existing tagger in Hall B at Jefferson Lab. The purpose of this beamtest will be threefold:

- To gain experience working with the final setup of the hardware under realistic experimental conditions
- To demonstrate that the calorimeter has the resolution we expect
- To show that the Monte Carlo simulation code developed for the FCAL is actually giving an adequate description of the calorimeter

In the following Section, details will be given on the basic setup of the FCAL, and in Section 2 the details of the proposed beamtest will be given. We note that for our beamtest, we plan to have data acquisition completely independent of the CLAS experiment, so that no "live" information from the CLAS datastream will be necessary on our end. We will give conclusions on our studies in Section 3.

1.1 Basic Setup of the FCAL

The Forward Calorimeter, or FCAL for short, is to be a major component of the upcoming GlueX Experiment in Hall D. The FCAL will consist of $2,800$ lead glass blocks, each with an individual PMT for detecting the Čerenkov light produced in the glass blocks as electromagnetic showers go through, and a high voltage Cockcroft-Walton base that can be controlled and monitored remotely. A schematic of the FCAL structure and its components is shown in Figure 1. The lead glass blocks themselves have dimensions $4 \times 4 \times 45$ cm, and together with the PMT and base, the total length of each module is approximately 1.00 m long.

The construction and development of each component of the FCAL has been done at Indiana University. The lead glass blocks themselves have been used in the past in other experiments, E852 at Brookhaven, and RadPhi using Hall B at Jefferson Lab. The Cockcroft-Walton bases are a new addition, and Indiana University has worked extensively on the design and testing of these bases. Currently, a sample of ~ 400 of these bases are being tested and monitored on high voltage for several months. One of the major goals in our beamtest is to gain experience in working with the final hardware setup for the FCAL, and understanding the characteristics of the components.

*kmoriya@indiana.edu
†mashephe@indiana.edu

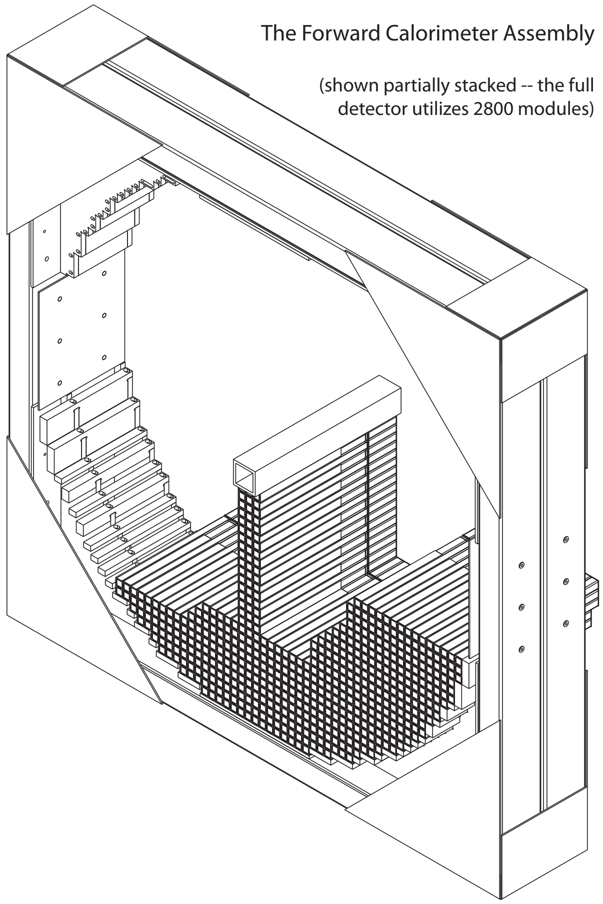

(a) Overview of the FCAL array.

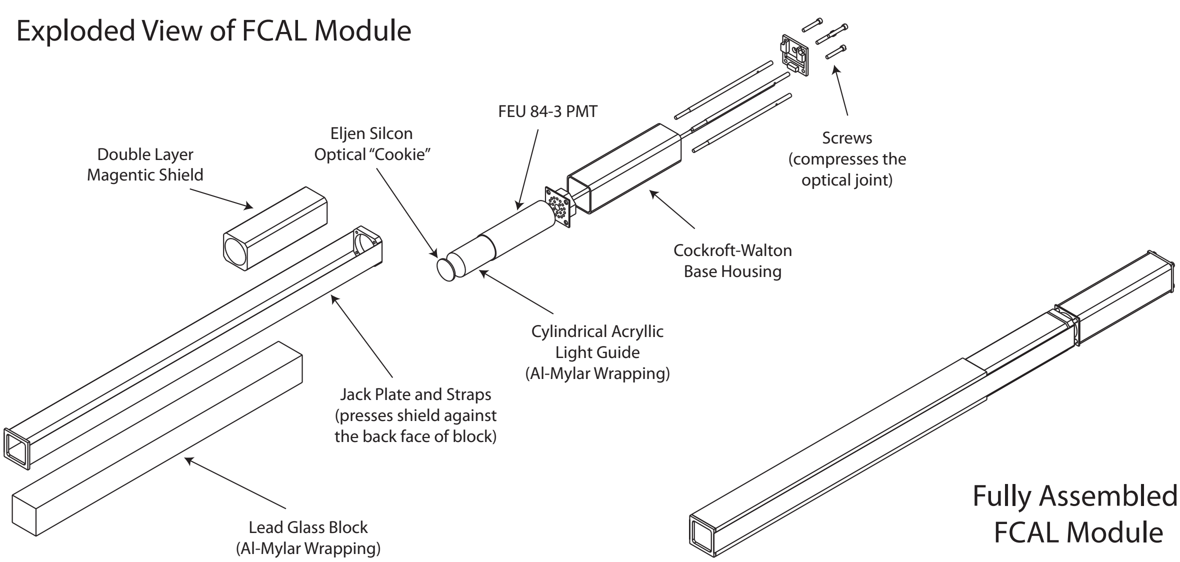

(b) Exploded view of each component.

Figure 1: (a) shows a partly stacked array of lead glass blocks for the FCAL. (b) shows an exploded view of each component of the FCAL.

Another component that will be introduced is the digital readout of the PMTs, which will rely on the newly developed flash analog to digital converters (fADCs) at JLab. The fADCs will have a sampling frequency of 250 MHz and a resolution of 12 bits. Together with the Cockcroft-Walton bases, testing that the fADCs work with the expected resolution is one of the goals of this beamtest.

1.2 Goals of the Beamtest

Presently, all of the necessary components for our proposed beamtest are available at Indiana University. Besides the hardware components mentioned above, the GlueX collaboration has been developing a GEANT-based Monte Carlo simulation of the GlueX detector [1]. A primary goal of our beamtest would be to test whether the timing and energy resolution of the FCAL is being modeled adequately with our current simulation. To test this, we hope to take data using a prototype of the FCAL at various energies and incidence angles. A detailed comparison of the actual data with the Monte Carlo simulation will then provide guidance on whether the model needs further refining.

According to past experimental results, the lead glass blocks to be used in the FCAL have the following resolution. For energy resolution, the RadPhi experiment quotes [2]

$$\sigma_E/E(\%) = 7.3/\sqrt{E[\text{GeV}]} \oplus 3.5 \tag{1}$$

from actual data taken from the experimental run, while Ref. [3] projects that with new optical couplings the statistical term in the above equation will be improved from 7.3% to 5.6%. A determination of the energy resolution will be an important part of our beamtest. Another point of interest will be to see what the low energy threshold of the detectors will be. This number is quoted as 30 MeV in Ref. [3], and the data taken from a beamtest will allow us to test this.

The timing resolution of the fADC readout has been studied in [4], and is $0.57 \pm 0.18(0.24 \pm 0.08)$ [ns] with 100 mV (500 mV) signal pulses. Our major goal for the beamtest will be an accurate estimation of these resolutions, and a comparison with our simulation model.

To recapitulate, the goals of the beamtest are to test the final hardware setup, to measure the various resolutions of the setup, and to compare this to the GEANT-based Monte Carlo simulation we have developed. In the next Section, we give the details of our proposal to test a prototype of the FCAL underneath the tagger in Hall B.

2 Details of Proposed Beamtest Underneath Hall B Tagger

In this Section we give details of a proposal to do a beamtest underneath the existing tagger used in Hall B. The basic setup of the FCAL prototype will be given, together with our plan on how to take data. We stress that our beamtest is being planned to run completely independent of the CLAS setup, and no live information from the CLAS datastream will be needed.

2.1 Calculation of Hall B Tagger Electron Trajectories

Our current plan for the beamtest is to do a measurement with a FCAL prototype underneath the tagger in Hall B. There is adequate space underneath the tagger to place an array of 5×5 blocks as a prototype of the FCAL. We have investigated the area underneath the tagger, and have built a simple model of the trajectory of the electrons that pass through the tagger system.

Figure 2 shows our simple model of the tagger system, with the electrons radiating a photon at the radiator. As a result, the electron has energy fraction E/E_0 where E_0 is the original energy of the electron given by the accelerator, and E is the final energy. The trajectory of the electron is completely determined by this fraction, and in Figure 2 we have plotted several electron trajectories based on their fractional energies.

According to our model, the electrons will bend through the tagger dipole magnet according to their respective momentum, and afterwards will follow a straight trajectory that can be calculated easily. Figure 3

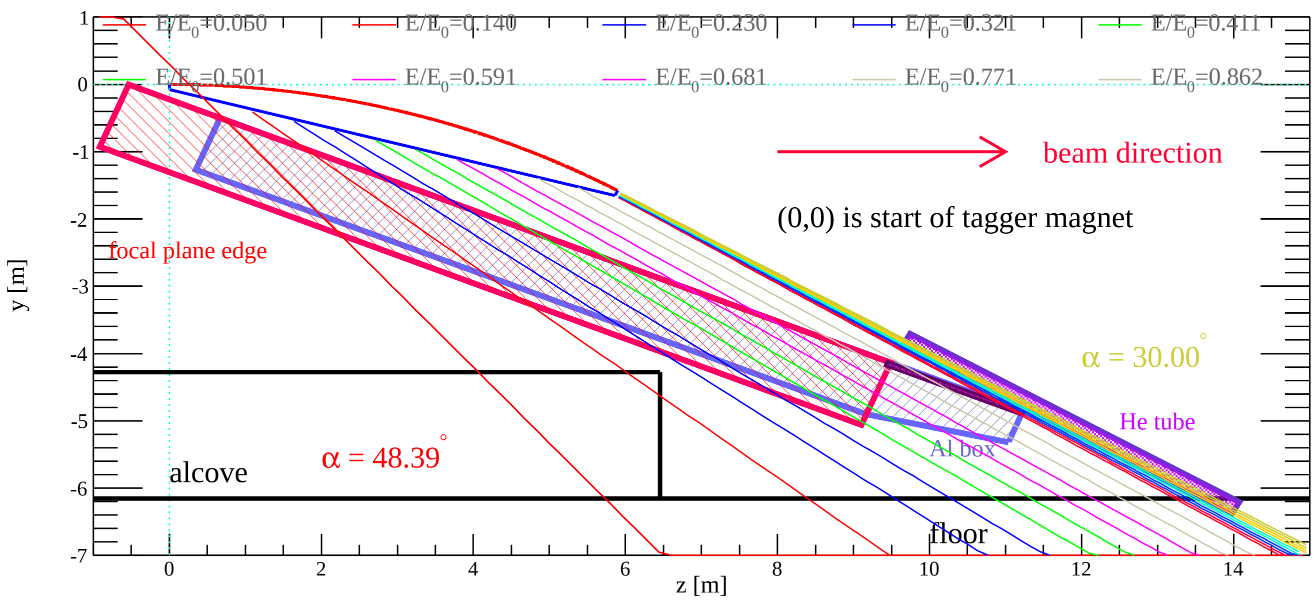

Figure 2: Our model of the tagger geometry. The beamline is along the horizontal (z) direction, and the vertical height is expressed as y, with the origin $(z, y) = (0, 0)$ being the starting point of the tagger dipole magnet. The lines correspond to various electron trajectories based on the energy fraction E/E_0, and various geometric objects such as the floor, alcove, and focal plane are shown. Also shown are the incident angles of the electron trajectories for the lowest and highest energy electron trajectories.

shows two configurations of a 5×5 array of lead glass blocks and how they will intersect the various electron trajectories when the prototype is placed on the floor, while Figure 4 shows the geometry when the prototype is placed in the tagger alcove, at a higher floor height. Currently, we are considering the tagger alcove as our first choice, since there seems to be less spatial constraints. If we are able to accumulate enough data within the tagger alcove and are still able to collect more data, several runs in the floor position may be considered. A potential location in this case may be at $z \sim 11.5$ m, where the tagger box has ended and there is some space.

With the various geometric constraints within the area, it seems that our prototype can only be placed within a range in z along the beamline from approximately 8 to 12 [m]. For a lower z coordinate further away from the beam dump, the electron energies are lower and statistics is also lower. For the tagger alcove (Figure 4), the same is true, and the further we are from the beam dump, the lower the energy and statistics.

A beamtest by fellow Hall D collaborators lead by Professor Richard Jones at the University of Conneticut was conducted in March 2010 in the floor area, with the help of Hall D scientists who are on-site. We assume their input will help us in determining the final position of the prototype.

2.2 Spread of Energies

As calibration of the energy resolution of the lead glass blocks is a crucial part of our beamtest, we are interested in the intrinsic spread of energies that will hit our prototype. Since we will not be connected to the CLAS live datastream, we cannot pick up coincidences with the CLAS tagger. However, we plan to have a scintillator paddle underneath the CLAS tagger paddles with known energy, and by taking a coincidence with this paddle, this will give us an independent measurement of the electron energies besides the position-dependence.

For each configuration of either floor or alcove, we can plot the ideal spread of the energy of the electrons

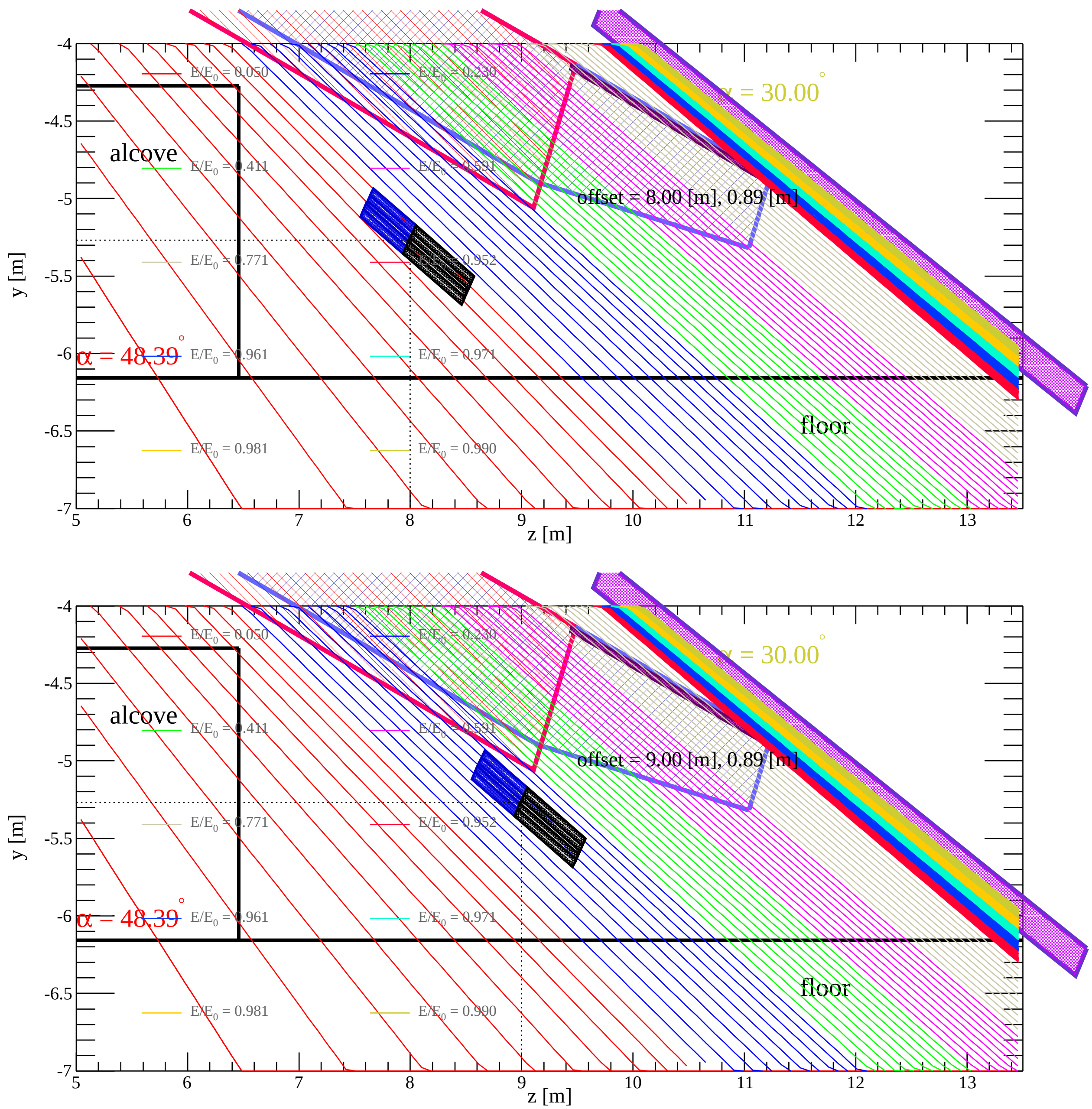

Figure 3: (a) shows a 5×5 array prototype FCAL (dark blue shaded blocks) centered at $z = 8.70$ [m], along with 60 [cm] long bases and support structures (gray shaded blocks). (b) shows the same prototype centered at $z = 11.70$ [m]. In both cases, the center of the array is offset by 0.89 [m] off of the floor, and the entire array is tilted at an angle of 32°. These dimensions are based on the support structure shown in Figure 9.

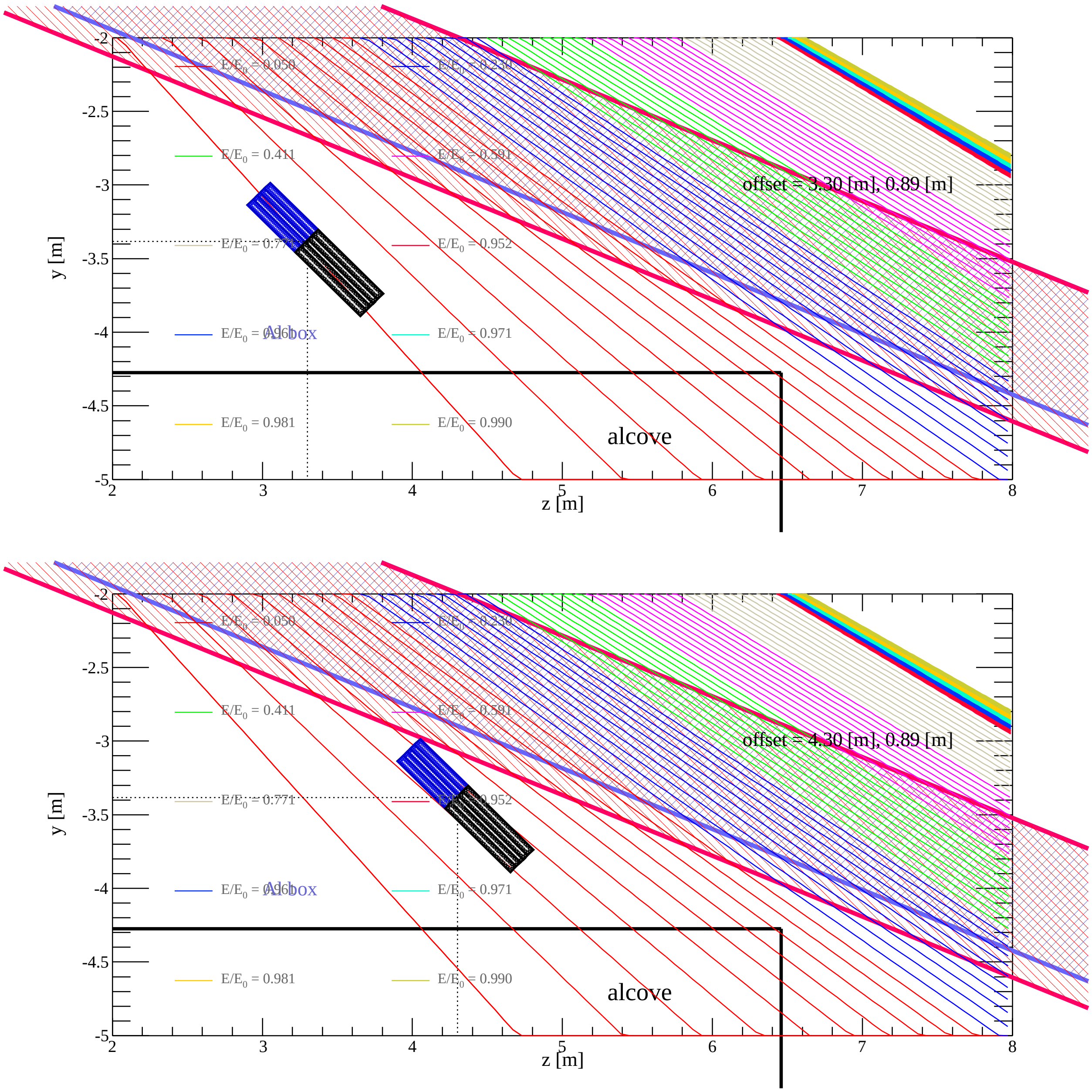

Figure 4: (a) shows a 5×5 array prototype FCAL (dark blue shaded blocks) centered at $z = 8.70$ [m], along with 60 [cm] long bases and support structures (gray shaded blocks). (b) shows the same prototype centered at $z = 11.70$ [m]. In both cases, the center of the array is offset by 0.89 [m] off of the alcove, and the entire array is tilted at an angle of 45°. These dimensions are based on the support structure shown in Figure 9.

that impinge upon the prototype. We plot these for the central lead glass block, and for a surrounding 5×5 array in Figure 5 (the justification for the 5×5 array is shown in the next subsection, § 2.3. The points of the graph represent the central values of the electron energies, and the error bars represent the full spread in energy across the entire array: the inner error bars the spread within the central block, and the outer error bars for the 5×5 array. We have chosen five different beam energies, $E_0 = 0.5 + 1.0 \times n$ ($n = 0, 1, 2, 3, 4$) to get an idea of what the central energies will be as a function of position, and also the spread in energies. From the figure we see that for example, by placing the prototype on the alcove at $z = 5$ [m], electron energies of 50 MeV up to 600 MeV could be obtained for different beam energies, and a beam energy of 1 GeV could be achieved if we are able to place our detector near the edge of the tagger alcove.

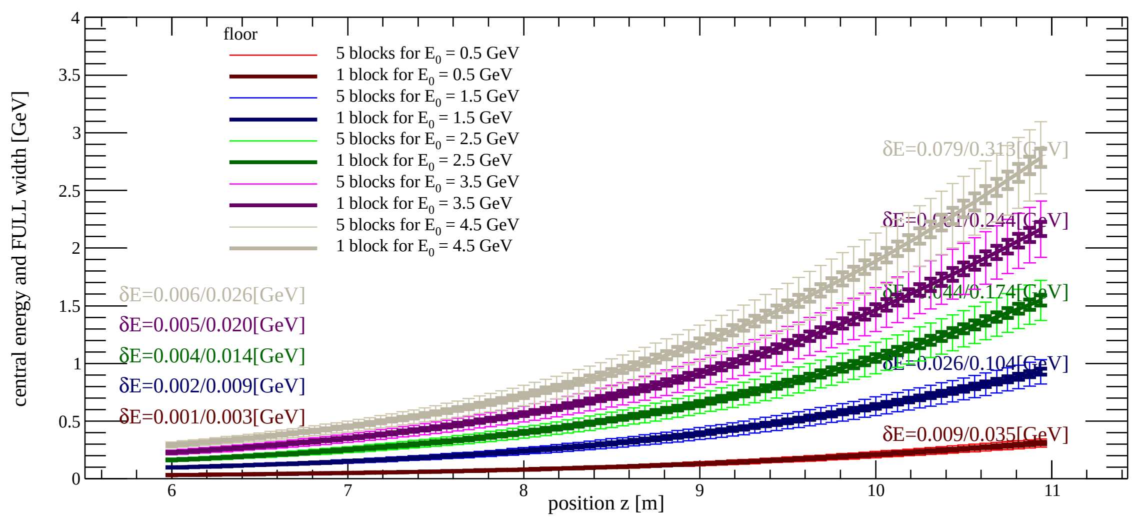

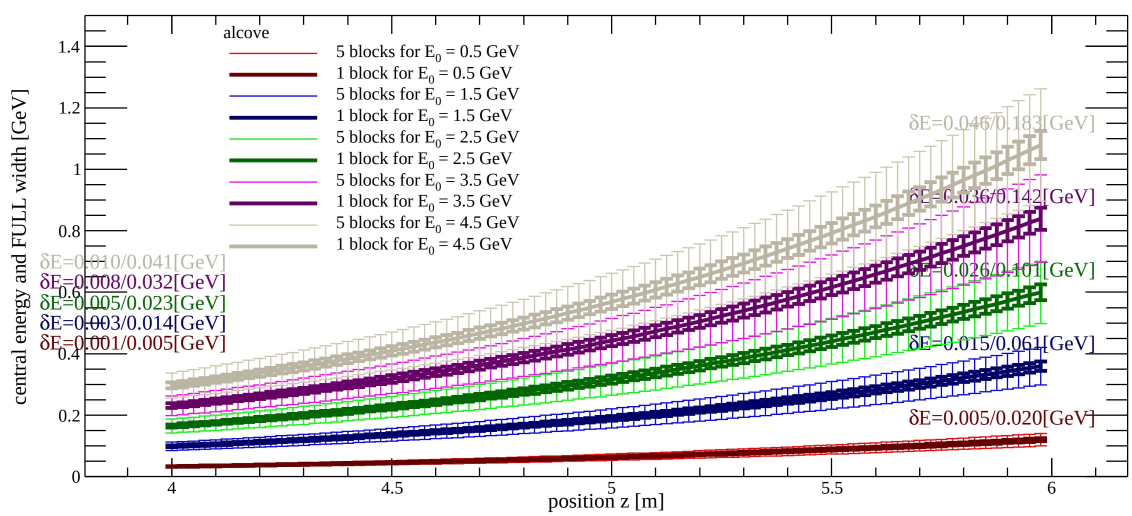

Figure 5: (a) shows the full spread in energy [GeV] for the central block (inner error bars) and 5×5 array (outer error bars) for different accelerator energies, represented by different colors. If we approximate the flux upon each 5×5 array as a constant flux, the RMS spread will be $\delta E_{\rm RMS} = \delta E/\sqrt{12}$. For reference, the values for the initial and final data points have been shown as text within the figure. The prototype has been placed on the floor level, with a tilt of 32°. (b) shows the same plot but with the prototype placed in the alcove with a tilt of 45°.

We can also calculate the fractional spread in the energy of the electrons around the central value of energy. Figure 6 shows this spread in energy normalized by the central energy value for various positions. The plot has been made for cases when the prototype is placed on the floor, or on the alcove. The fractional spread in energy is roughly between 1.4% and 2.3% of the central value when the prototype is on the floor, and between 1.4% and 4.2% when placed on the alcove. The higher fraction on the alcove is due to the energies of the electons being lower in the alcove.

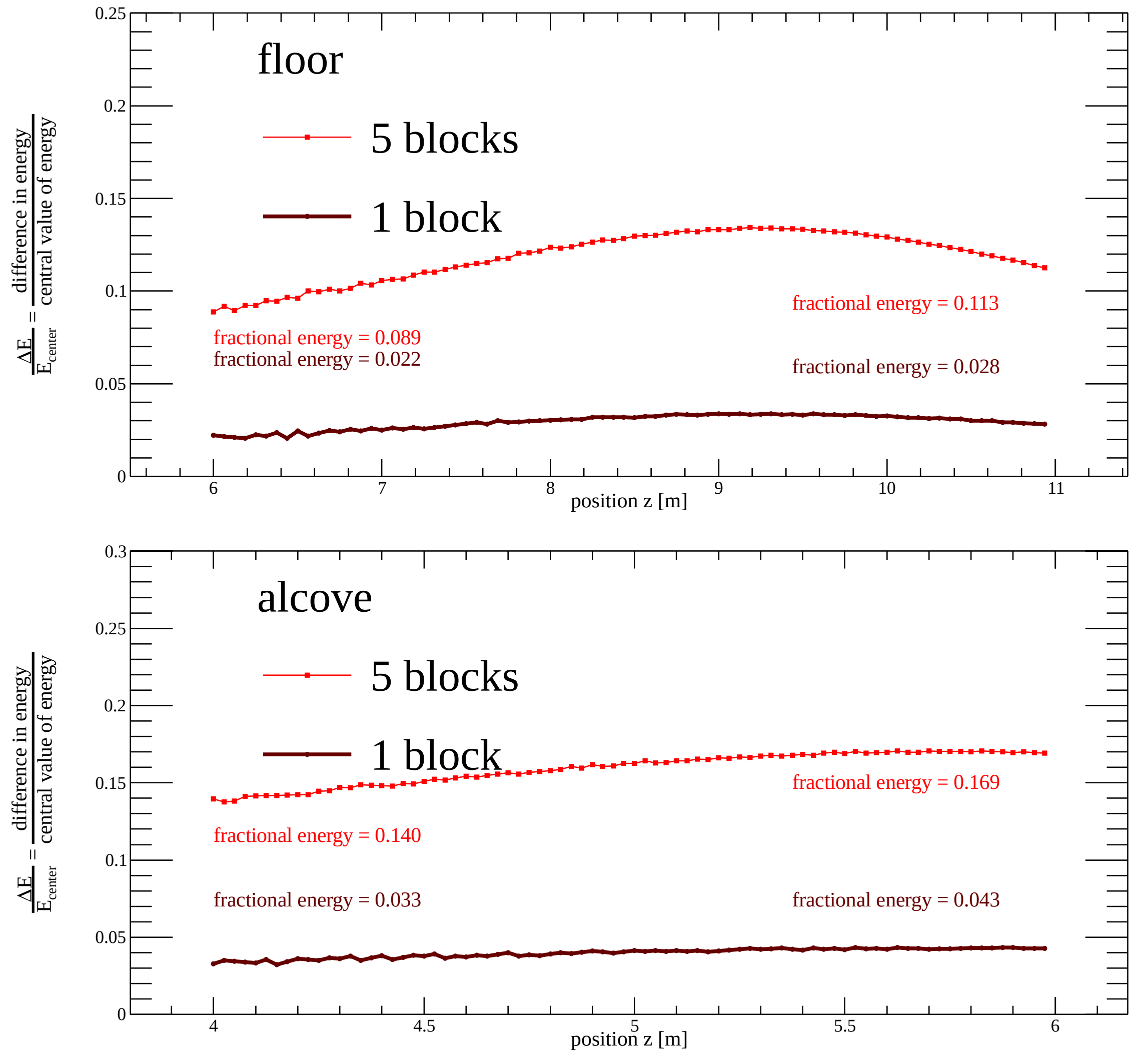

Figure 6: (a) shows the full spread in energy as a fraction of the central value for the central block (dark red points) and 5×5 array (red points). In this plot, the numbers do not change with accelerator energy. The prototype has been placed on the floor level, with a tilt of 32°. For reference, the fractional energies at the lowest and highest z positions are shown in text. (b) shows the same plot but with the prototype placed in the alcove with a tilt of 45°.

The standard energy resolution for a calorimeter is of the form of Equation 1, and we see that with an intrinsic spread in energy of less than $\sim 3\%$, this is sufficient to determine the resolution of the calorimeter by correcting for the effects of the intrinsic spread of the electron beam on the central block.

Clearly, Figure 6 shows that we cannot take all electrons that hit a 5×5 array, since the spread in fractional energy is greater than the resolution expected by our prototype. To accomodate this we plan to have a plastic scintillator trigger on the central 3×3 array of lead glass blocks, and similarly a veto scintillator on the surrounding blocks. In the offline analysis we will be able to pick up coincidences and decide which block the electron had initially hit, and the expected spread in energy will be much less than our resolution. Further details of this trigger will be shown in the § 2.4.

In the next section, we use a GEANT simulation to study how many blocks we need to measure the incident energy of the electrons to the precision necessary for our calibration.

2.3 GEANT-based Simulation

To ensure that our 5×5 array is sufficient to measure the energies of the electrons incident on it, we used a GEANT4 simulation of the FCAL to determine how many blocks were necessary to capture most of the incident energy. The simulation was set up with an electron beam incident on the central block of a 15×15 array, and the deposited energy was summed within blocks of $n \times n$ from the central block, with $n = 1, 3, 5, 7, 9, 11, 13, 15$. The results for a small sample of energy bins are shown in Figure 7 for representative energies of $E_{e^-} = 0.1, 0.5, 1.0, 1.5, 2.0, 2.5, 3.0, 3.5$ GeV. In all cases, the central block on which the initial electron is incident upon absorbs more than 90% of the incident energy, and including the surrounding blocks to make a 3×3 array leads to more than 96% of the incident energy. Figure 8 shows a summary of the fraction of energies absorbed by each array, for energies ranging from 0.1 GeV to 4.0 GeV in increments of 0.1 GeV, for array sizes of 1×1, 3×3, 5×5, and 7×7. The central values of the graphs are the mean values of the fractional energy contained in each array, and the error bars represent the RMS spread. We see that beyond the 3×3 array, there is not much gain in energy by increasing the size of the array; there is almost no gain in absorbed energy by going beyond a 5×5 array. From this study we conclude that for the energies currently available at CLAS, a 5×5 array is sufficient to enclose each shower that is created by the initial electron. Figures 7 and 8 were made with $20,000$ events incident at each energy.

2.4 Configuration of Prototype

We plan to configure our 5×5 array prototype at various positions along the dispersion direction of the tagger magnet, and also at various incident angles to determine whether or not we can correct for showers entering the array away from normal angles. To achieve this, we plan to build a support structure that can be arranged to different positions along the beamline and also at various tilting angles. A preliminary sketch of this support structure is shown in Figure 9. This will be approximately 1.85 m along the beamline, 0.76 m across, and 1.00 m in height, and when placed in the tagger alcove will be able to absorb electron energy fractions of $E/E_0 = 0.05$ to ~ 0.15. By manually positioning the support structure along the beamline, we will be able to collect electrons that differ in energy by a factor of ~ 3.

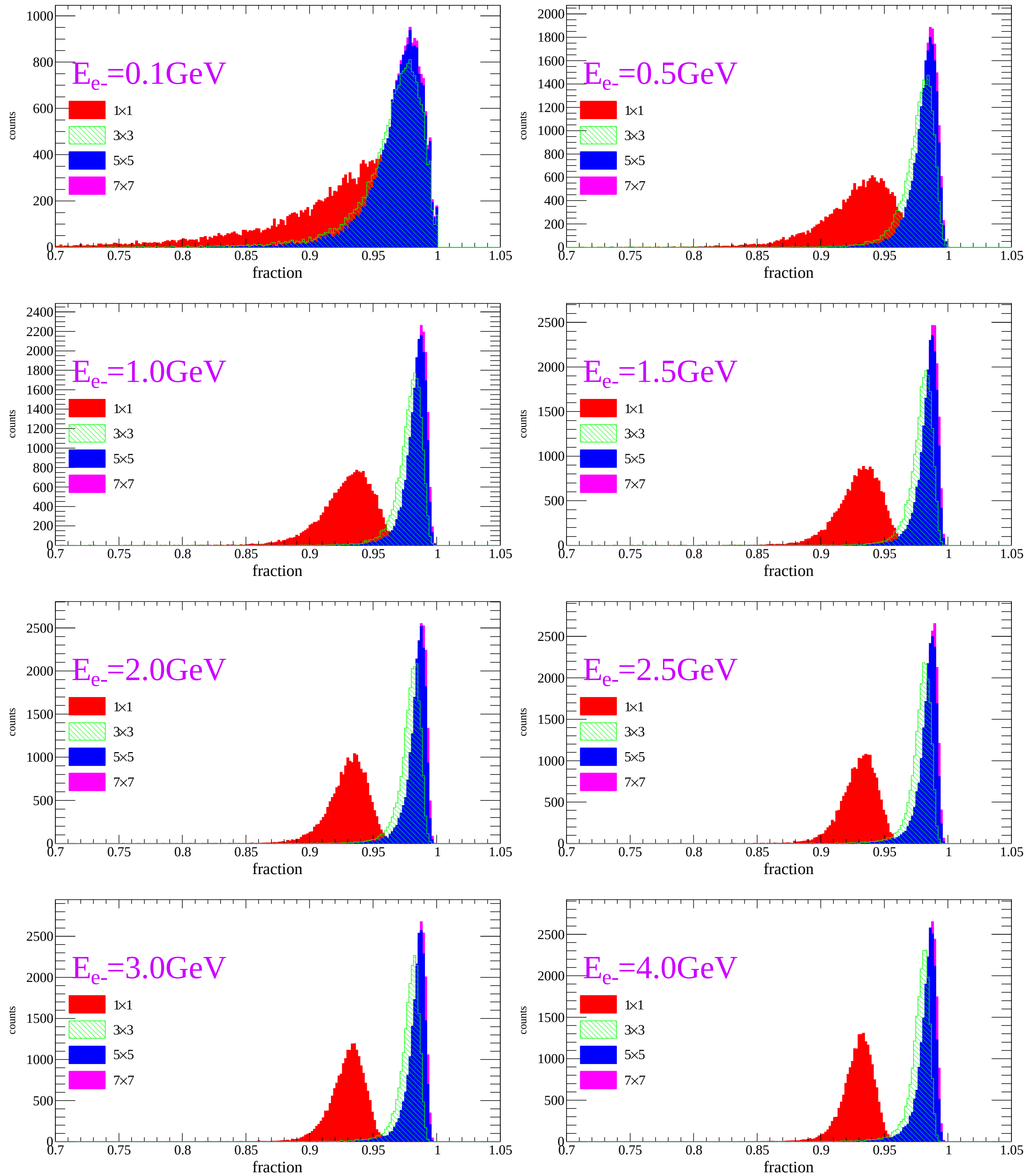

Figure 7: The fractional amount of absorbed energies for various initial e^- energies by an $n \times n$ array of lead glass blocks, where $n = 1, 3, 5, 7$. The initial e^- was incident on the central block, and the total energy absorbed by the surrounding $n \times n$ array is shown as the different colors. We see that in all cases the central block (red filled) absorbs over 90% of the energy, and together with the surrounding 3×3 array (shaded green), this accounts for most of the energy deposited. There is a small increase in the energy absorbed by the 5×5 array (filled blue), but there is almost no difference when going to a 7×7 array (filled magenta). Therefore we come to the conclusion that a 5×5 array is sufficient to absorb the necessary energy to do a calibration test. Note also how the spread in energies absorbed by the central block becomes smaller for higher electron energies.

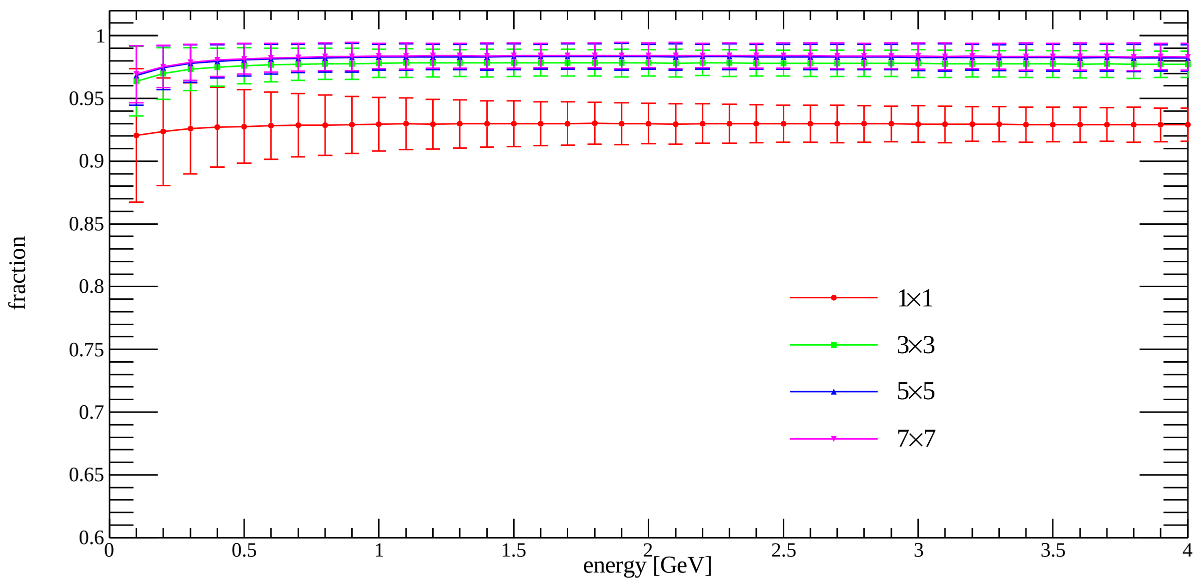

Figure 8: The fraction of energy captured by the $n \times n$ blocks ($n = 1, 3, 5, 7$) as a function of energy. The values and error bars of this figure are taken as the mean and RMS values of Figure 7. The fraction of the energy deposited in the central block, normalized to the initial electron energy, is shown as the red circles. There is a slight increase in the energy we capture when increasing the array from 3×3 (green squares) to 5×5 (blue upward triangles), but this is indistinguishable with a 7×7 array (magenta downward triangles), so we conclude that a 5×5 array is sufficient for our studies.

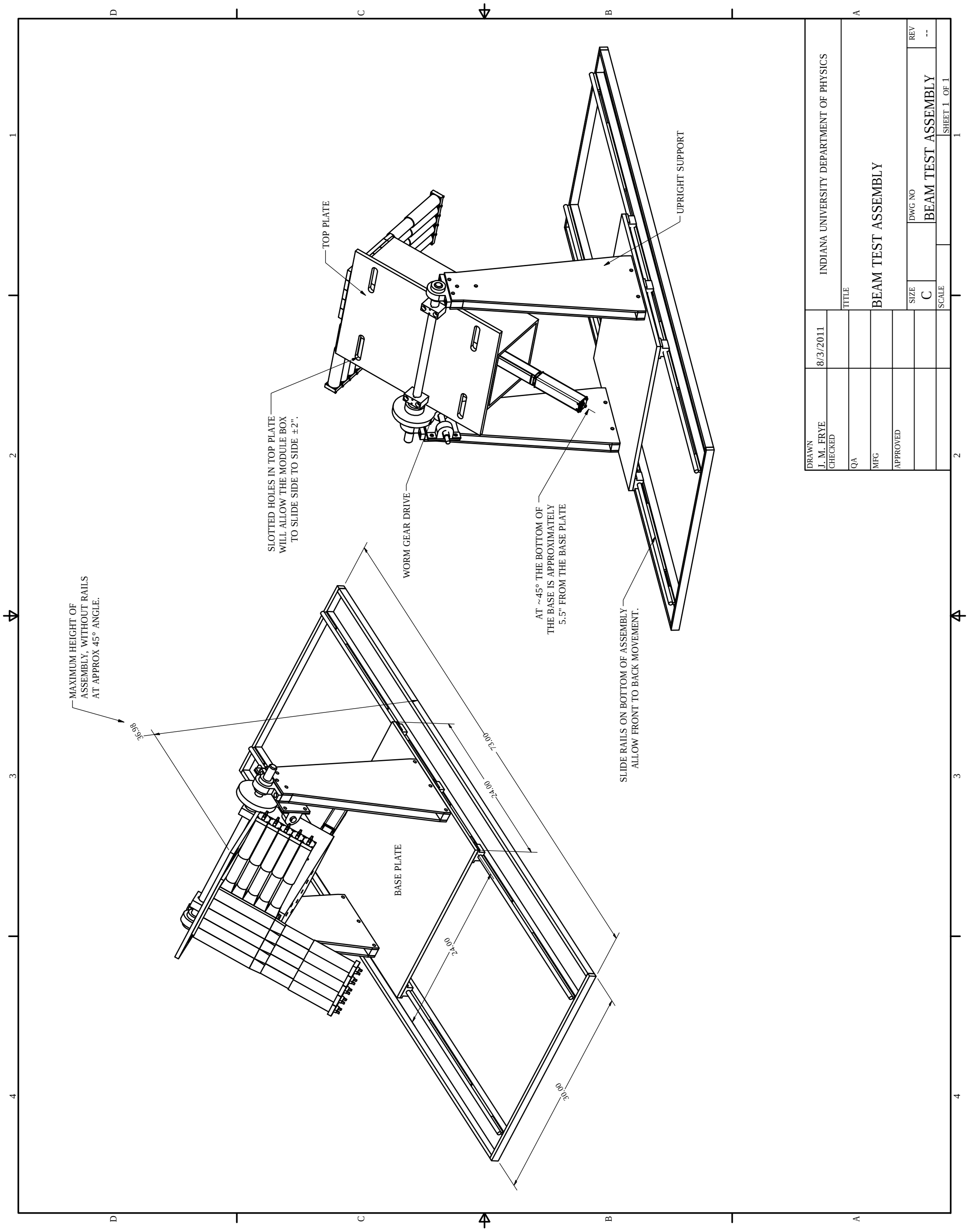

Figure 9: A drawing of the assembly we plan to use for the beamtest. The assembly will hold the 5×5 array of lead glass blocks, and the associated PMTs, HV supplies, etc. It is built so that movement along both the beamline and transverse directions are possible, as well as being able to tilt the array at various angles. The width of the assembly is approximately 73 inches (1.85 m) along the beamline, 30 inches (0.762 m) transverse to the beamline, and has a height of ~ 40 inches (0.939 m) including the rails when tilted at an angle of 45°.

For our trigger, we plan to have small scintillator paddles in front of each lead glass block, and an electronics trigger will be constructed. Currently we are working on a scheme where one array of five scintillators will be placed horintally, and one array of five scintillators will be placed vertically (Figure 10). The central three blocks in each array will have an OR coincidence, while there will be a veto coincidence on the blocks on the edge blocks since we will not be able to fully reconstruct the showers centered on the edge blocks. Each of the scintillator paddles in the two arrays will have an associated FEU-84-3 PMT, CockcroftWalton base, μ-metal shielding and acrylic light guide. Figure 11 shows a diagram of the electronics logic. The final trigger will be an AND of both central scintillator array signals and a VETO from all edges. The scalers connected to each array will allow us to estimate how well our beam is centered on our prototype. Also, as mentioned at the beginning of § 2.2, coincidences with an independent scintillator paddle placed underneath the CLAS tagger paddles of known energies will allow us to independently confirm the energies of the electrons. Discussions are ongoing with Alexander Somov, Elton Smith, and Hovanes Egiyan at JLab about the trigger and use of fADCs.

The 5×5 array we envision will be helpful also when we are trying to determine the calibration constants of each module in the array, since we can choose 9 different combinations of a 3×3 array within the entire configuration. Using the various trigger signals and a Monte Carlo simulation of the energy distribution within the blocks, we will be able to determine these calibration constants.

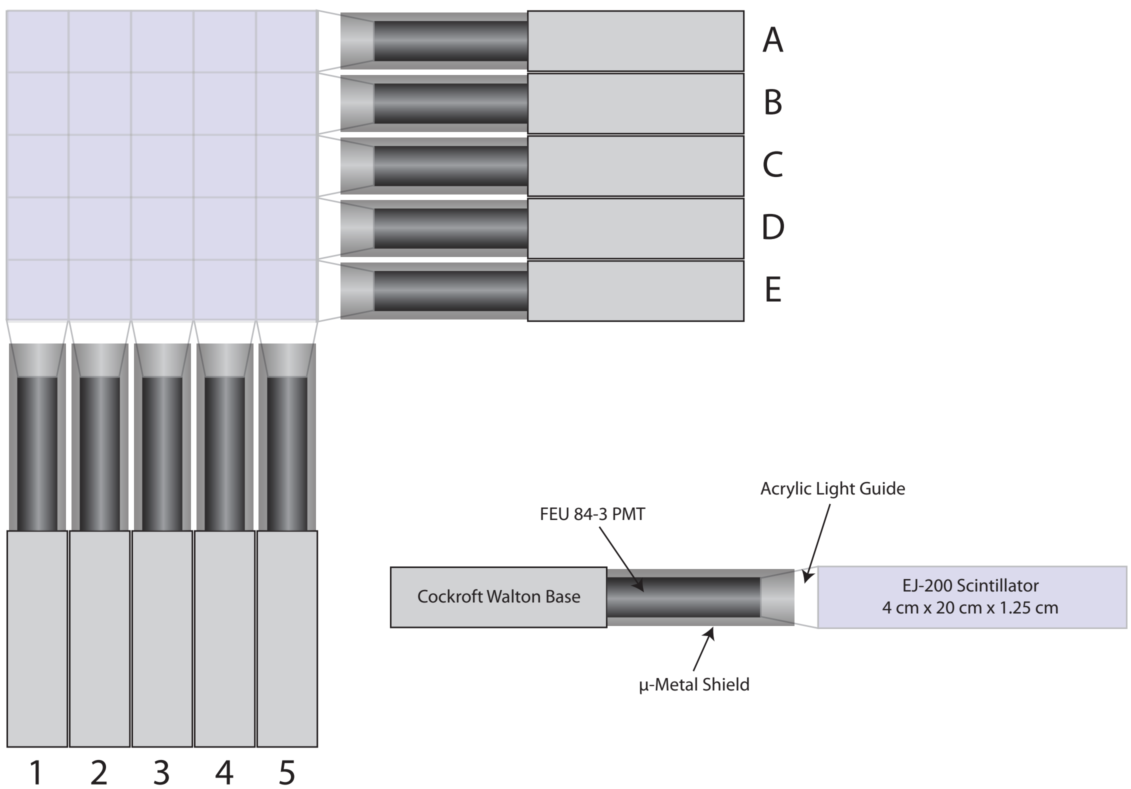

Figure 10: A schematic of two arrays of scintillators to be used as the trigger. Each array will have five scintillator paddles, one in the horizontal and one in the vertical direction.

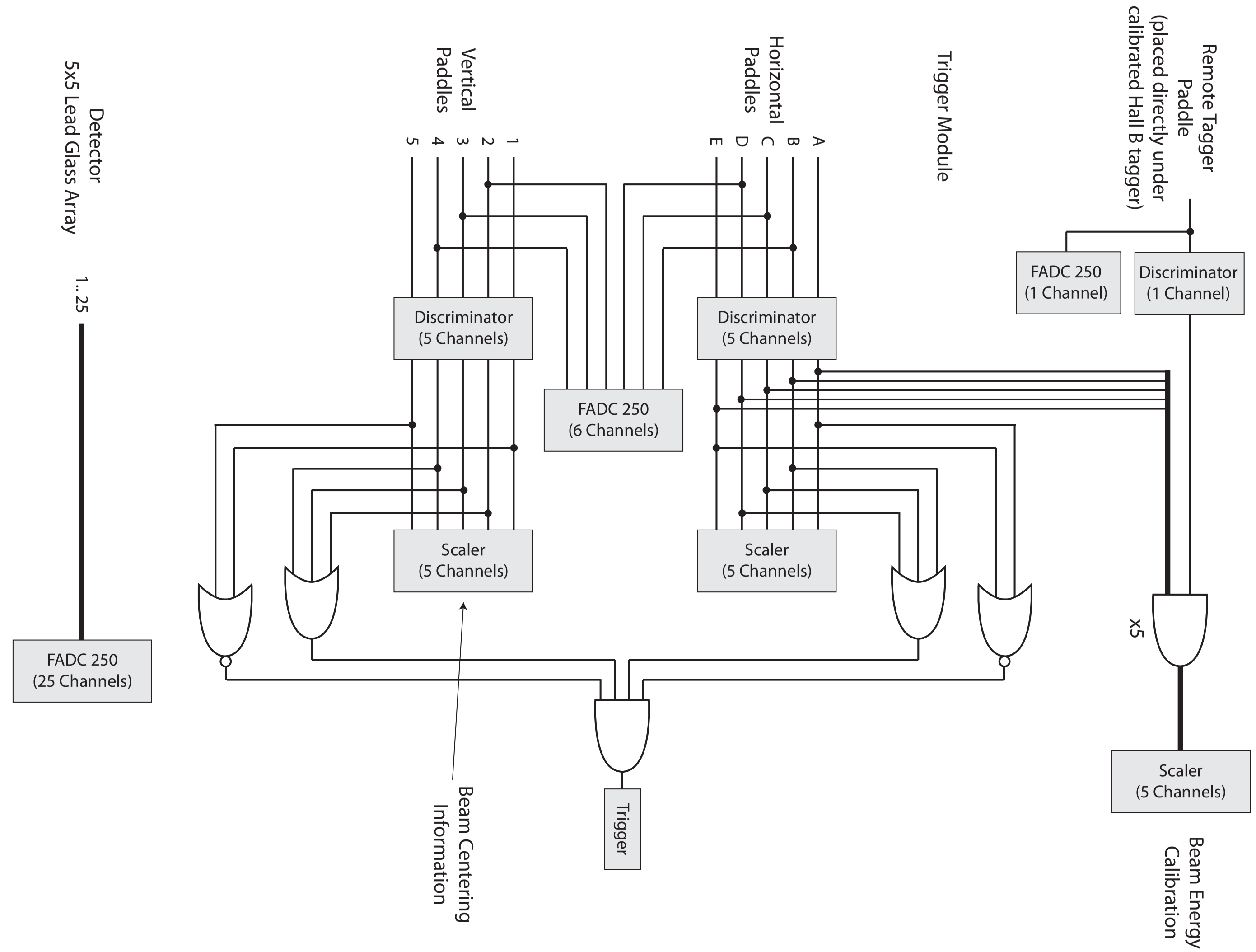

Figure 11: The electronics logic to be used in the trigger. The central three scintillators in each array will be have an OR coincidence, and a VETO will be placed on the two scintillators on the edges. The final trigger is an AND of the two centers and a VETO on all edges.

For our data acquisition, a dedicated DAQ will be made ready by Indiana University and Hall D scientists at JLab for data taking completely independent of CLAS. The minimum electronics required for our beamtest is as follows:

- 32 channels for fADC
- 11 discriminator channels with 2 outputs each
- 15 scaler channels
- 1 quad logic Fan-In/Fan-Out module (LeCroy 429A or equivalent)
- 1 four-fold and 5 two-fold coincidence units (two Phillips 755 or equivalent)

2.5 Consideration of CLAS Running Conditions

We plan to conduct our proposed beamtest during the fall 2011 run of CLAS, which will be running HDICE. Currently, the run will utilize the 2-, 3-, and 4-pass energies, which is convenient for us since we would like to take measurements at various energies. The proposed CLAS run conditions are as follows:

- beam duration:
  - November 19, 2011 (Sat) – December 22, 2011 (Thu)
  - January 5, 2012 (Thu) – May 13, 2012 (Sun) (start of year long shutdown)
- beam energy: 3/4/5 pass
- beam current: 30 nA ???
- Master OR (MOR) rate for tagger: 20 MHz ???
- radiator: Au, 4×10^{-4} radiation lengths ???

With these run conditions, and with the geometric setup shown, we expect to have electron rates of higher than several kHz if a trigger is placed on our central block. To simulate the rates, we calculated the relative intensity of electrons assuming that for a nominal bremsstrahlung process, the energy distribution follows $\mathrm{d}N/\mathrm{d}E_\gamma \propto 1/E_\gamma$. Figure 12 shows the relative rates for the electron energies that will be detected by the CLAS tagger. On the right of this plot are the absolute rates, normalized to a total tagger Master OR rate of 20 MHz. We see that for a trigger in front of the central block, a rate of several kHz is easily reachable.

Since the plots in Figure 8 were made with only $20,000$ events for each energy, we see that accumulating the same statistics as the Monte Carlo simulation is achievable in a very short time, and we should be able to accumulate sufficient statistics at a single electron energy and angle within a few running hours at most. Depending on the run conditions of Hall B and how frequently we will be able to have access to the Hall, we should be able to collect data at numerous points over a period of several weeks. We note from Figure 12 that due to the energy distribution, we have a higher rate at higher energies of the electrons. This is advantageous for accumulating higher statistics, but at the higher energies, the spread in energy also becomes larger, so there is a tradeoff of statistics and beam energy resolution.

For the cleanliness of our events, we have consulted Eugene Pasyuk of the CLAS collaboration. We have been informed that the electrons pass through the CLAS tagger scintillators, *i.e.*, the so-called E-counters and T-counters, which are 4 mm and 20 mm thick respectively, but besides these, there is only a very thin aluminum window and air that the electrons pass through. Effects such as multiple scattering and energy loss due to these materials can be simulated if necessary.

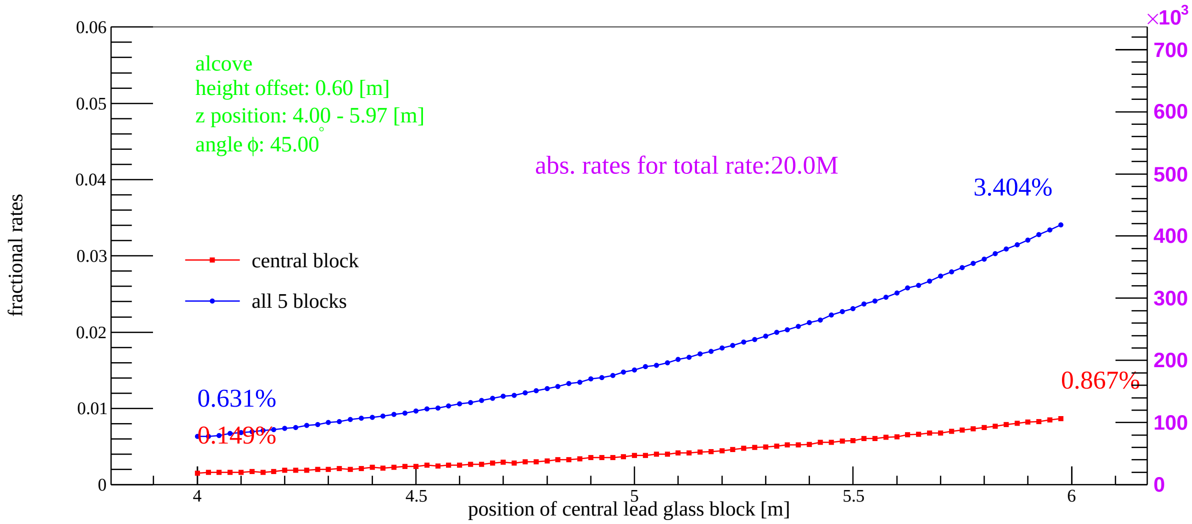

Figure 12: The expected relative rates as a function of electron energy. The bremsstrahlung distribution is assumed to be proportional to $1/E_\gamma$ where E_γ is the radiated photon energy. The red data points are for the central block, and the blue points are for the 5×5 array. The right axis shows the absolute rates, normalized to a total Master OR rate of 20 MHz. We see that for our central block, a rate of more than a kHz is achievable.

3 Conclusion

In this document we have given an overview of our proposal to conduct a beamtest of a prototype of the Hall D Forward Calorimeter (FCAL) underneath the Hall B tagger. The datataking will be done completely independent of the CLAS data acquisition, and we aim to calibrate the FCAL at different energies. With a high Master OR rate of ~ 20 MHz on the CLAS tagger, we should be able to accumulate sufficient statistics to do a calibration within several hours for each position once the detector has been correctly set. Depending on how many times we are able to access the hall and how many times the endpoint energy of the accelerator is changed, a few weeks of datataking should enable us to test the FCAL resolution at various energies and angles, and also test the limits of the hardware setup.

References

[1] "The GlueX Wiki", `http://www.jlab.org/Hall-D/software/wiki/index.php/Main_Page` .

[2] R. T. Jones *et al.*, "A bootstrap method for gain calibration and resolution determination of a lead-glass calorimeter", Nucl. Instrum. Meth. **A566**, 366 (2006).

[3] Alex R. Dzierba, Matthew Shepherd, Beni Zihlmann, "GlueX/Hall D Calorimeter Final Design and Safety Review", GlueX doc 988-v1, available online at the GlueX Wiki [1].

[4] J. V. Bennett, M. Kornicer, M. R. Shepherd, and M. M. Ito, "Precision timing measurement of phototube pulses using a flash analog-to-digital converter", Nucl. Instrum. Meth. **A622**, 225 (2010), arXiv:1005.5349 [physics.ins-det] .